New Hobby Eberly telescope metrology systems: design, implementation, and on-sky performance

Lee, Hanshin, Hill, Gary, Drory, Niv, Vattiat, Brian, Ramsey, Jason, et al.

Hanshin Lee, Gary J. Hill, Niv Drory, Brian L. Vattiat, Jason Ramsey, Randy Bryant, Matthew Shetrone, Stephen Odewahn, Sergey Rostopchin, Martin Landriau, Jim Fowler, Ron Leck, Herman Kriel, George Damm, "New Hobby Eberly telescope metrology systems: design, implementation, and on-sky performance," Proc. SPIE 10700, Ground-based and Airborne Telescopes VII, 107002B (6 July 2018); doi: 10.1117/12.2314138

SPIE.

Event: SPIE Astronomical Telescopes + Instrumentation, 2018, Austin, Texas, United States

New Hobby Eberly Telescope Metrology Systems: Design, Implementation, and On-sky Performance

Hanshin Lee[a], Gary J. Hill[a], Niv Drory[a], Brian L. Vattiat[a], Jason Ramsey[a], Randy Bryant[b], Matthew Shetrone[b], Stephen Odewahn[b], Sergey Rostopchin[b], Martin Landriau[a], Jim Fowler[b], Ron Leck[a], Herman Kriel[b], George Damm[b]

[a] McDonald Observatory, University of Texas at Austin, 2515 Speedway, C1402, Austin, TX, USA 78712-0259;
[b] Hobby-Eberly Telescope, University of Texas at Austin

ABSTRACT

The Hobby-Eberly Telescope is an innovative 10-meter telescope, located at the McDonald Observatory. We have completed a major multi-year upgrade of the HET that has substantially increased the field of view to 22 arcminutes by replacing the optical corrector, tracker, and prime focus instrument package and by developing a new telescope control and metrology systems. The metrology systems include four independent optical sensors to provide fully redundant alignment and pointing information to keep the telescope aligned to within a few microns and a few arc seconds. We detail the design, implementation, on-sky performance, and lessons learned.

Keywords: Hobby-Eberly Telescope, HET, Metrology System, Tip tilt, Distance measuring, Wavefront sensor, Guider

1. INTRODUCTION

The Hobby-Eberly Telescope (HET) is an innovative fixed altitude telescope with 10-meter diameter segmented aperture, located in West Texas at the McDonald Observatory. We have completed a major multi-year upgrade of the HET that has substantially increased the field of view (FOV) to 22 arcminutes by replacing the optical corrector, tracker, and prime focus instrument package and by developing a new telescope control and metrology systems. As the tracker carries the corrector and the instrument package to follow the sidereal motion, the new metrology systems provide a real time active control of the optical alignment between the corrector-instrument package and the telescope primary mirror.

The metrology systems include one tip/tilt sensor (TTS), one distance measuring interferometer (DMI), two guide probes (GP), and three wavefront sensors (WFS). Both the TTS and DMI use a 1500nm laser return off of a primary mirror segment to monitor the mechanical alignment of the telescope in the tip / tilt / focus axes. The GPs and WFS use stars over annular field area between 8 and 11 arcmin radius. Each GP has 22x22 arcsec^2 FOV and uses the centroid information of a guide star to provide the overall telescope pointing feedback as well as additional information on the transparency and image quality. Each WFS has 5 arcsec diameter FOV with 11 sub-apertures across the telescope pupil to measure the telescope wavefront map. The low order wavefront aberration terms (tip/tilt/focus/coma) are used to provide optical alignment feedback in all degrees-of-freedom of the telescope. These individual systems collectively provide fully redundant optical alignment and pointing information for the telescope to the telescope control software to maintain the telescope alignment to within a few microns in linear axes and a few arc seconds in angular axes over a 4-meter long track with temperature and gravity changes. We begin this paper with an overview of the HET metrology system hardware designs and describe the implementation of both the hardware and software of the metrology systems. We then present the on-sky performance of these systems by showing a couple example control loop data collected last year.

2. OVERVIEW OF METROLOGY SYSTEMS

Due to the intrinsic operational nature of the HET, the electro-opto-mechanical payload at the top of the telescope must be constantly moved around in order to track the sidereal motion. Hence, at any given moment, the payload system can potentially be out of alignment with respect to the fixed primary mirror of the HET. In order to maintain the image quality, the alignment of the payload system needs to be maintained to the accuracy as shown in the table below.

Ground-based and Airborne Telescopes VII, edited by Heather K. Marshall, Jason Spyromilio, Proc. of SPIE Vol. 10700, 107002B · © 2018 SPIE
CCC code: 0277-786X/18/$18 · doi: 10.1117/12.2314138

Table 1. The allowed ranges of misalignments of the WFC.

Alignment parameters	Decenter	Defocus	Tip/tilt	Rho
Requirement at 1-σ level	±10μm	±10μm	±4arcsec.	±20arcsec.

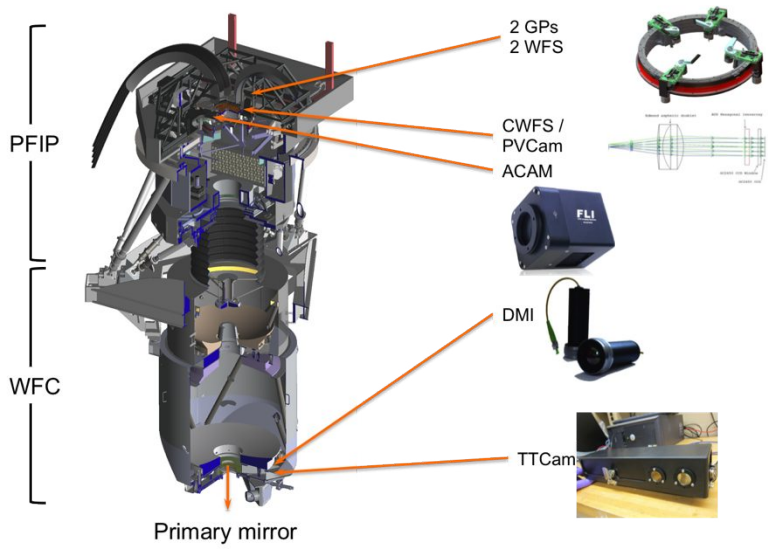

Figure 1 The overview of the WFU metrology systems.

The feedback to keep these alignment specifications requires robust metrology and we developed and deployed the following closed-loop metrology subsystems for this:

✓ Guide probes (GP): Monitoring the position on the sky, plus plate scale of the optical system, and monitor the image quality and atmospheric transparency plus field rotation correction.

✓ Wavefront sensors (WFS): Monitoring the plate-scale, focus, and tilt of the WFC.

✓ Distance measuring interferometer (DMI): Monitoring the physical distance between the WFC and primary mirror.

✓ Tip-Tilt Camera (TTCam): Monitoring the physical tip/tilt of the WFC with respect to the optical axis of the primary mirror.

✓ Acquisition Camera (ACAM): For initial field identification, telescope pointing.

The wavefront sensor is a newly introduced metrology system to the HET in order to close the loop on all axes of the system together with the DMI and TTCam adapted from the current tracker metrology system. Both operate at a near infrared wavelength[5]. These systems provide redundancy for the highest possible reliability in monitoring the alignment of the WFC. The DMI and TTCam measurements are directly related to the alignment state of the mechanical structure of the WFC, while responses from the WFS and GP are analyzed to determine the "*optical*" alignment state of the WFC, which is ultimately what we care about. The WFS analysis is based on the following alignment–aberration relations. Decenter of the WFC causes systematic wavefront tilts across the field. This is equivalent to the telescope pointing error and equivalent to the stellar position measurement from the GP. Tilt errors add field constant coma to the aberration field of the WFC, while the axial motion introduces defocus aberration that is also field constant. The defocus aberration, however, can also be produced when the global radius of curvature (GRoC) of M1 changes. As this variation can also produce plate scale variation, an appropriate monitoring system is necessary. Although the Segment Alignment Maintenance System (SAMS) maintains the positions of the 91 mirror segments with respect to each other [6], it is less sensitive to the GRoC change. Thus, we monitor the GRoC variation by the combination of focus position from the WFS with the physical distance measurement from the DMI. The feedback from the SAMS can be used as a redundant piece of information on the GRoC change. The primary mirror tip/tilt is currently controlled by the Mirror Alignment Recovery System (MARS). MARS maintains the segment tip/tilt to an accuracy of 0.14 arc-seconds rms[7]. We continue using this system for the WFU. The DMI, TTCam, GP, and WFS systems currently provide fully redundant closed-loop alignment and pointing information for the telescope, thereby keeping the WFC in focus and suppressing alignment-driven field aberrations.

In addition, there is a pupil-viewing camera (PVCam) and a calibration wavefront sensor (CWFS). The PVCam images the telescope pupil (therefore the M1 segments and the moving baffle at the exit pupil of the WFC). The CWFS will have denser sub-apertures than the WFS will have. This enables finer sampling of the telescope wavefront error and thus provides reference signals against which the WFS are calibrated.

On the HET, the optical alignment of the WFC with respect to the M1 must be held dynamically while the image moves as much as 3.8 m with respect to the main telescope structure along the M1 focal sphere. The mechanisms controlling the tracker synthesize the required tracker motions along the focal sphere by a combination of X, Y, focus

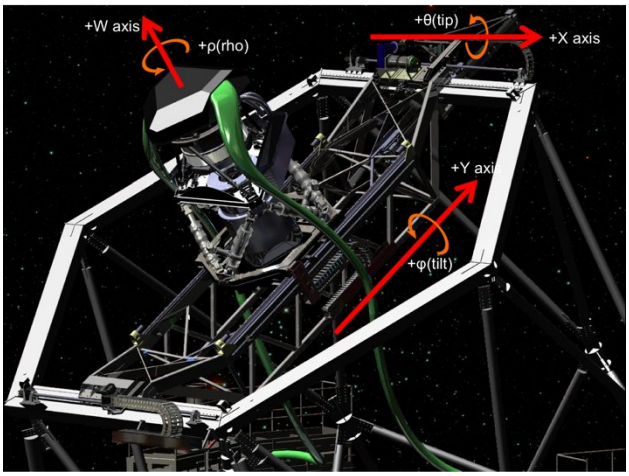

Figure 2 WFU Coordinate system.

(W), tip (θ), tilt (ϕ), rotation (ρ) axes of stacked X and Y stages, a hexapod system and a rotation stage. The range of motion for each axis is: 3.8 m in x and y, 130 mm in z, 17° in θ and ϕ, and 44° deg in ρ (Figure 2). In the very original design of the telescope the only feedback to control the motion with respect to the M1 was provided by a guider, which constrained only the two pointing degrees of freedom. The remaining degrees of freedom were to be modeled. To overcome the deficiencies of the mount-models, additional metrology systems were added to provide feedback on focus, and tip and tilt of the corrector with respect to M1. Focus is measured with an absolute distance measuring interferometer (DMI) while tip and tilt are measured with an auto-collimator system called the tip/tilt camera (TTCam)[4]. Both the DMI and TTCam operate at a wavelength of 1.55 μm that is outside the range of any current or planned instrument used on the HET. These two systems are to be directly adopted for the same metrology in the WFU. In order to close the alignment control loop on all axes for the WFU, we have added wavefront sensors to the suite of metrology systems. In conjunction with the guide probes, the WFS provides direct information on the *optical alignment state* of the WFC. For the purpose of calibrating the WFS, the CWFS will also be installed. For the M1 mirror segment reflectance monitor, the PVCam will be used. The individual metrology sub-systems are detailed below.

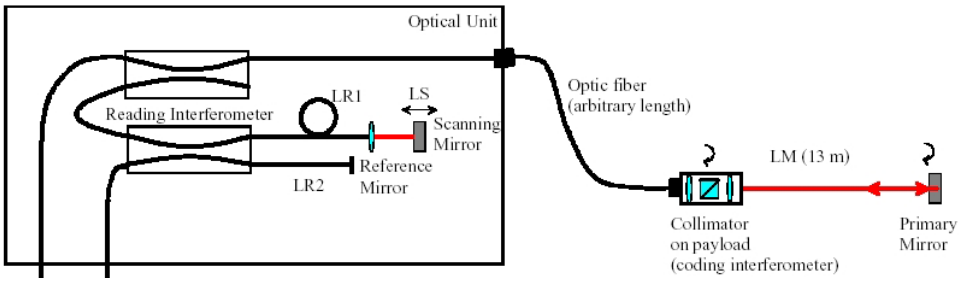

Figure 3 The operation principle of the distance measuring interferometer.

2.1 Distance Measuring Interferometer (DMI)

The DMI is a low-coherence distance measuring interferometer developed by Fogale-Nanotech[8]. The system operation is based on a pair of Michelson interferometers where all of the optical paths, except the measurement arm, are along optical fibers (Figure 3). The first interferometer encodes the phase difference to the primary mirror with respect to a reference at the collimator measurement head, a distance equal to 2LM. The two arms of the second interferometer induce phase delays of 2(LR1+LS) and LR2 respectively. Here, LS can be adjusted by an optically encoded scanning mirror. The second interferometer reads the phase difference from the coding interferometer by scanning through the exact phase matching condition where LR1+LS-LR2 = LM. The system light source is a polychromatic super-luminescent diode (SLED). An interference signal is detected only when the phase difference is less than the coherence length of the source and is modulated by a peaked function called the visibility curve. Figure 4 shows an example of an interference curve. The peak of the

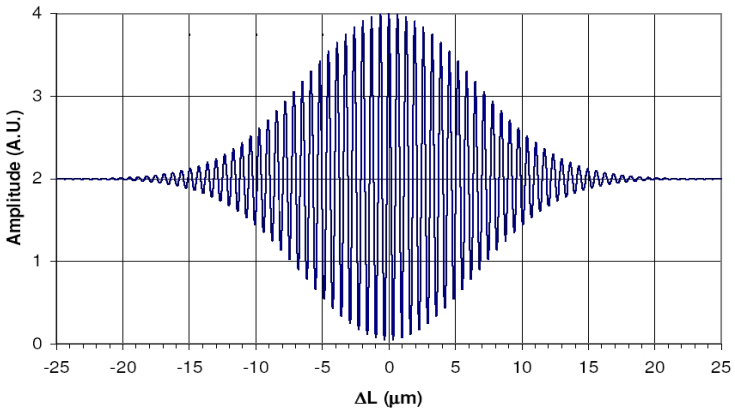

Figure 4 An example interference curve. The peak of the visibility curve occurs at the exact phase matching condition of LR1+LS-LR2 = LM. The absolute distance is obtained by finding the peak.

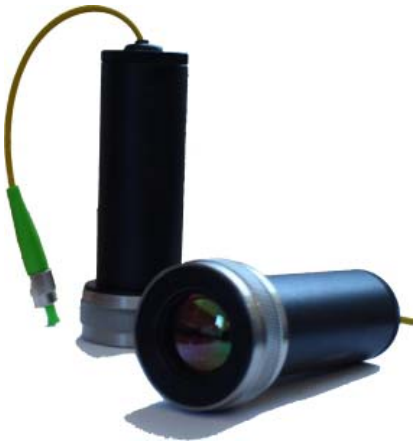

Figure 5 The DMI measurement heads with a focusing lens at the output end of the head.

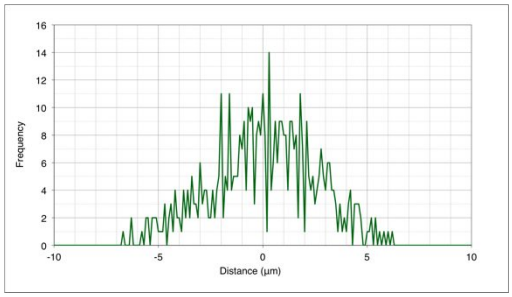

Figure 6 The repeatability measurement of the current HET DMI.

visibility curve occurs at the exact phase matching condition of LR1+LS-LR2 = LM. This configuration allows the compact measurement head (Figure 5) of the instrument to be mounted remotely. The length of the optical fiber feeding the measurement head can be arbitrary and the distance measurement is unaffected by thermally induced changes to the length of feed fiber. The reading interferometer is housed in a thermally controlled chamber to maintain stability. The absolute distance is obtained by finding the peak. The range of the scanning mirror is 40 mm. This allows a sufficiently wide range for locating and setup of the measurement head that can be scanned in 5 sec. The scanning range is in fact narrower than 40 mm to reduce the measurement time. The visibility curve is sampled in 10ms. The RMS repeatability of measurements is 2.5 μm over time scales several minutes (Figure 6). The long-term accuracy is specified at 1ppm[8].

The system currently installed at the HET has two channels: one is to measure a nominal distance of approximately 12.6 m, located at the current corrector, and used for tracker metrology, and the other channel is set to measure a nominal distance of approximately 26.2m to measure distances at the center of curvature of the primary mirror. For the WFU, we plan to add two more DMI heads, thus three DMI heads sharing one two-channel DMI source. The DMI heads are to be located within the WFC in such a way that we can measure physical distances between the WFC and all mirror segments and the piston map of the entire M1 mirror segments can be obtained, which is otherwise difficult with only one DMI on the WFC. Each head will have its optical axis passing through the center of curvature (CoC) of the M1. This approach is expected to make a better correction to the M1 mirror segment piston errors.

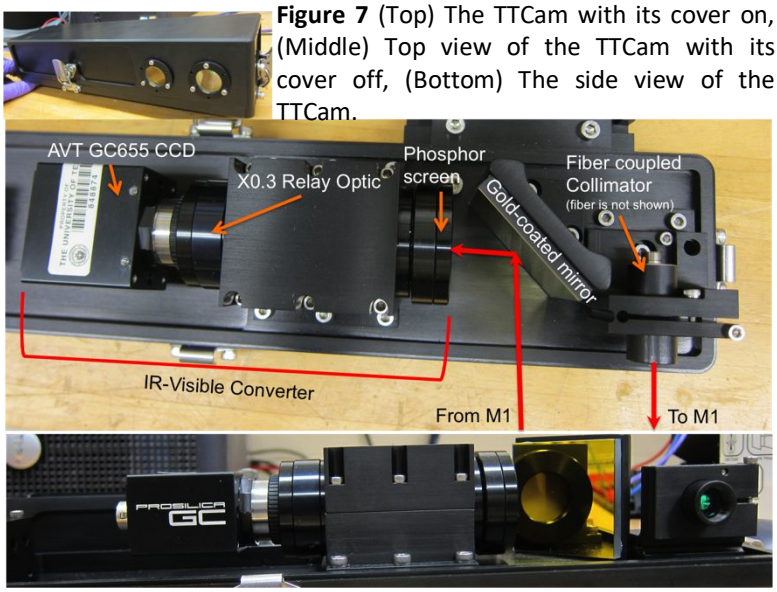

Figure 7 (Top) The TTCam with its cover on, (Middle) Top view of the TTCam with its cover off, (Bottom) The side view of the TTCam.

2.2 Tip Tilt Camera (TTCam)

The basic design concept of the new TTCam (as shown in Figure 7) is similar to the current one. The TTCam consists of a fiber-coupled light source and a collimator. The light source is an amplified spontaneous emission (ASE) source from Lightwaves2020. The source has the central wavelength at 1.55 μm with a spectral width of approximately 50 nm, which eliminates problems with fringing due to a laser source and forms a smooth Gaussian-like PSF. The collimated beam passes through a window and then focused by a mirror segment on reflection. The beam optical axis is slightly tilted so that the returned beam makes an angle with respect to the collimated beam. The return beam passes through another window. The beam is then folded by a gold-coated fold mirror to an IR converter with a camera attached (Edmund Optics). The converter has a phosphor screen where the returned beam is focused. The IR spot on the screen is then

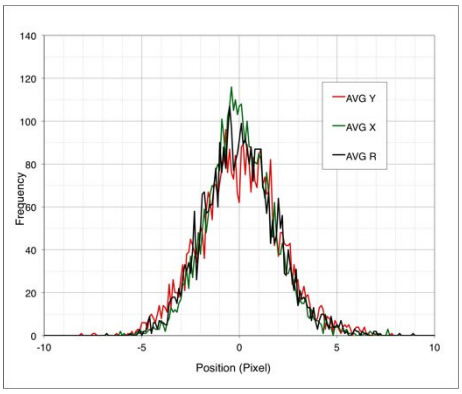

Figure 8 The repeatability measurement of the current HET TTCam. The pixel scale is 0.145 arc-seconds.

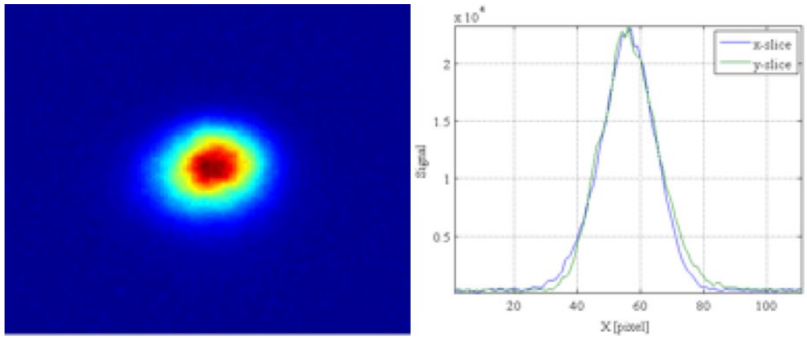

Figure 9 (Left) The spot imaged through the IR-Visble converter and (Right) Horizontal and vertical slices of the spot.

converted into a visible spot so that the camera can reimage it onto a machine vision CCD sensor (Allied Vision Technology (AVT) Prosilica GC655, 659×493 pixels, 9.9µm pixel, 12bit). The magnification is ×0.33 therefore the capture range of the TTCam is 160×120 sq. arc-seconds. The entire TTCam assembly will be mounted to the side of the M3 strong back of the WFC.

The TTCam installed in the current corrector was developed in house due to the lack of a commercial product operating in the near infra-red which met our specifications for accuracy, stability and capture range[5]. The current TTCam projects a collimated beam at a normal to the primary mirror and the return beam is focused by a mirror segment and steered by a beam-splitter to a camera with a phosphor coated CCD yielding a spot size of 2 mm. The current TTCam has a capture range of 150 arc-seconds and rms repeatability of 0.3 arc-seconds (Figure 8). In a previous prototype with the same IR-Visible converter and light source[4], we have measured the image centroid stability (Figure 9). The stability in the current test setup is less than a tenth of a pixel. The source power of 0.8 mW produces sufficiently high signal-to-noise ratio (SNR ~ 3800).

2.3 Guide Probe (GP) and Wavefront Sensor (WFS)

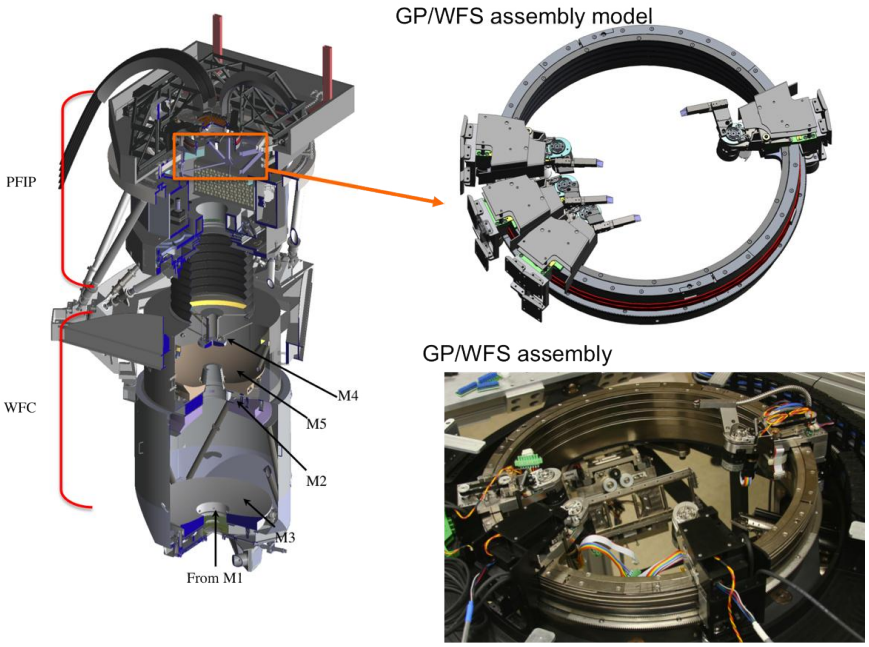

Figure 10 (Left) A section view of the WFC and PFIP where the guide probe and wavefront sensor assembly reside near the focal surface (marked by orange rectangle near the top of the PFIP). (Top right) A close-up view of the guide probe

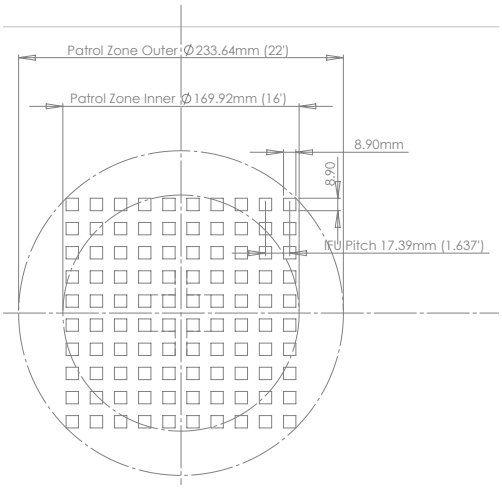

Figure 11 The layout of the WFU focal plane and the metrology service field.

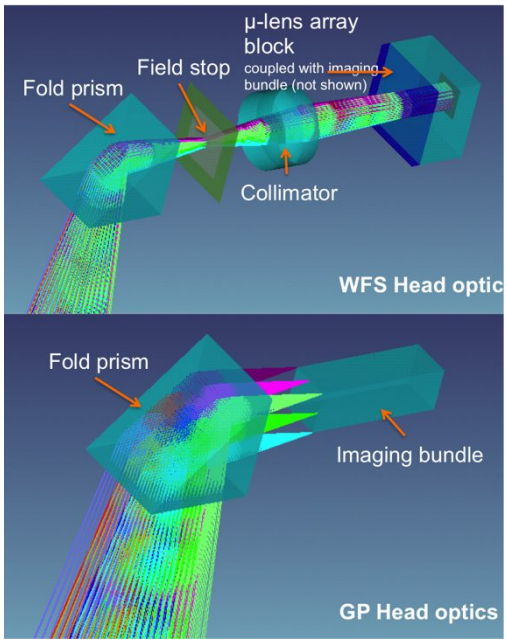

Figure 12 The WFS and GP head optics optical models.

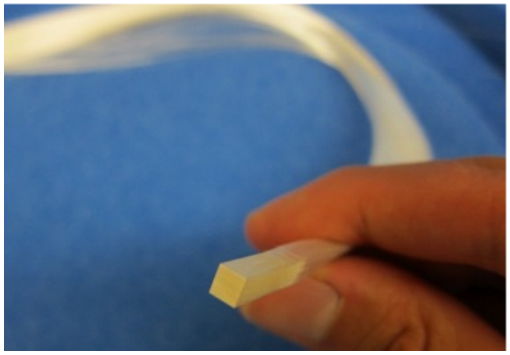

Figure 13 The imaging fiber bundle used in the GP/WFS assembly.

and wavefront sensor assembly where two guide probes and two wavefront sensor probes are mounted on a circular bearing; each probe has a probing arm; a folding prism is at the tip of each arm, steering the beam from the WFC to an imaging fiber bundle (guide probe) or to a collimation lens that feeds a collimated beam to a lenslet array butted to an imaging fiber bundle (wavefront sensor) (optical components are not shown). (Bottom right) The actual GP/WFS assembly under construction is shown.

Figure 10 illustrates the layout of the WFC and Prime-Focus Instrumentation Package (PFIP). The guide-probe (GP) and wavefront sensor (WFS) assembly resides near the focal surface assembly marked by an orange rectangle near the top of the PFIP. A close-up view of the GP/WFS assembly model is shown on the top right and the actual assembly under construction and test is shown at the bottom of Figure 10.

There are four probes; two are GP and two are WFS probes. Each GP and WFS probe patrols the metrology service field in the WFU focal plane (i.e. an annular field from 16' to 22' diameter, see Figure 11). Each probe has its own head optics in the GP/WFS assembly (Figure 12). A folding prism is placed at the tip of the head i) to route the beam within the metrology service field into a pupil imaging optics that forms Shack-Hartmann (SH) spots on an imaging fiber bundle for WFS or ii) to directly feed an imaging fiber bundle for GP. The imaging fiber bundles transmit stellar images (for GP) or a SH image (for WFS) to the output systems located in a remote electronic box of the PFIP. The field stop in the WFS head defines a field of view of 4.5 x 4.5 sq. arc-seconds. The GP field of view is defined by the size of the input matrix of the imaging bundle (4x4 sq. mm or 22.6x22.6 sq. arc-seconds on the sky) (Figure 13). At the time of this writing, we are procuring the imaging bundles from Schott.

Each imaging bundle feeds an output system that consists of a relay optic and a CCD sensor (Figure 14). In the GP, the beam speed at the input end of the imaging bundle is f/3.65. It has been measured that the beam speed at the output end of the imaging bundle is f/2 due to the focal ratio degradation (FRD) [9]. Therefore, the relay optics in the GP output system is designed to be able to accept f/2 beams. There are total 6 spherical lens elements (2 doublets and 2 singlets) in each GP relay system (Jenoptik fabricated the lenses). The relay system converts f/2 into f/3, thus x1.5 magnification. The GP output relay is equipped with a set of Johnson B, Sloan g, r, i, and clear filters so that the GP measurements can be used as additional flux calibration inputs for the HETDEX science data calibration. The CCD sensor is Finger Lakes Imaging (FLI) Microline MLx285 that uses a Sony ICX285AL monochromatic 16-bit CCD chip. The pixel format is 1434x1050 with 6.45μm pitch. The pixel scale of the GP is 0.024 arc-second per pixel, thus we plan to bin by 8 times at least. The recorded stellar images in the GP are analyzed to determine the centroids and thus the correction to the telescope pointing, to assess the image quality, and to monitor the telescope plate scale variation. The guide star image will also be used to determine atmospheric transparency and to generate flux calibration

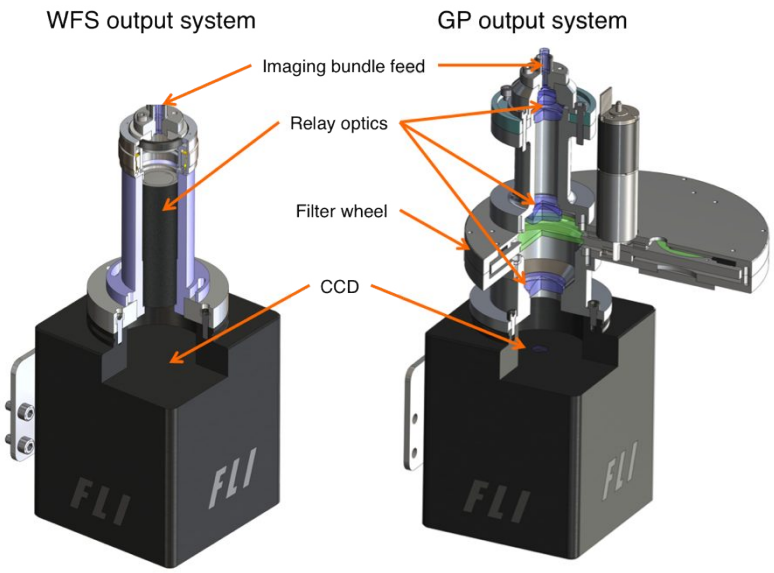

Figure 14 The WFS and GP output system section view.

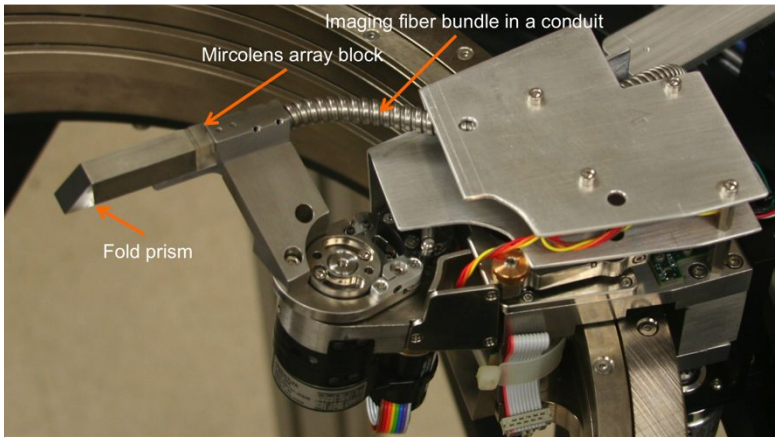

Figure 15 One of the assembled WFS probe head in the GP/WFS assembly.

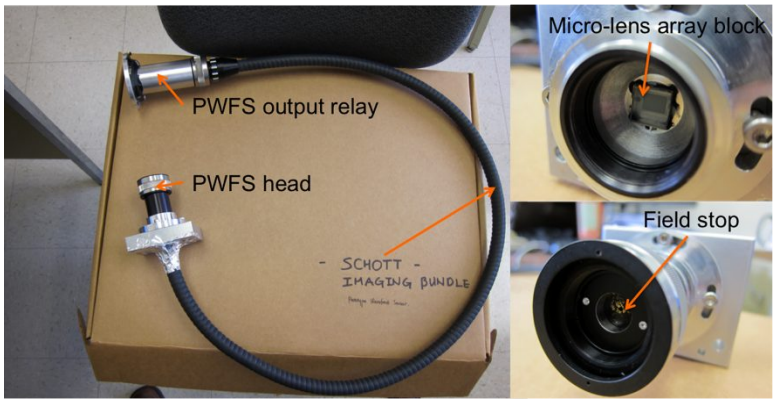

Figure 16 The solid model of the Prototype-WFS.

data for the HETDEX science data reduction. The expected guiding accuracy is 0.25 arc-seconds with 0.1 arc-seconds as a goal. One of the assembled WFS head is shown in Figure 15. It shows the folding prism at the tip of the probe followed by a field stop and collimation lens (not shown) in side the rectangular housing. The micro-lens array block is glued to the end of the housing. The side surfaces of the micro-lens array block will be painted. The imaging fiber bundle (inside the metal conduit) is glued to the exit face of the micron-lens array block.

In the WFS, each sub-aperture feeds the imaging bundle at f/16. Our lab measurement indicated that, at this input speed, the output beam comes out at f/4.5 or slower due to FRD in the imaging bundle. We have identified an off-the-shelf 1:1 f/4 finite-conjugate relay system from Edmund Optics as a suitable output relay optic for the WFS. We have successfully used this relay in a prototype WFS (PWFS, see below for further descriptions). The WFS operates without filters and uses the same FLI Microline CCD. The sub-aperture grid is 11x11 and, at any given tracker position, at least 45 sub-apertures are in full or partial illumination. This allows us to determine the first 22 Zernike aberration coefficients (or up to radial order 6), among which the first 7 terms are explicitly used to determine the correction to the WFC alignment, in particular focus and tip/tilt. The WFS can reach SNR ~ 70 in a 60sec exposure for m_v=18 stars with 5e- rms read noise. This can lead to 0.07 arc-seconds SH spot centroid accuracy in rms at a worst case. The expected intrinsic WFC alignment estimation accuracy from the WFS is ±1.5 μm in decenter, ±2.5 μm in focus, ±0.7 arc-seconds in tip/tilt, and ±1.5 arc-seconds in rho in peak-to-valley[10]. Ideally, we wish to have stars for two guide probes and two wavefront sensors, each operating in one quadrant of the metrology service field, but the current baseline is to have at least two guide stars and one wavefront sensor star.

2.4 Acquisition Camera (ACAM)

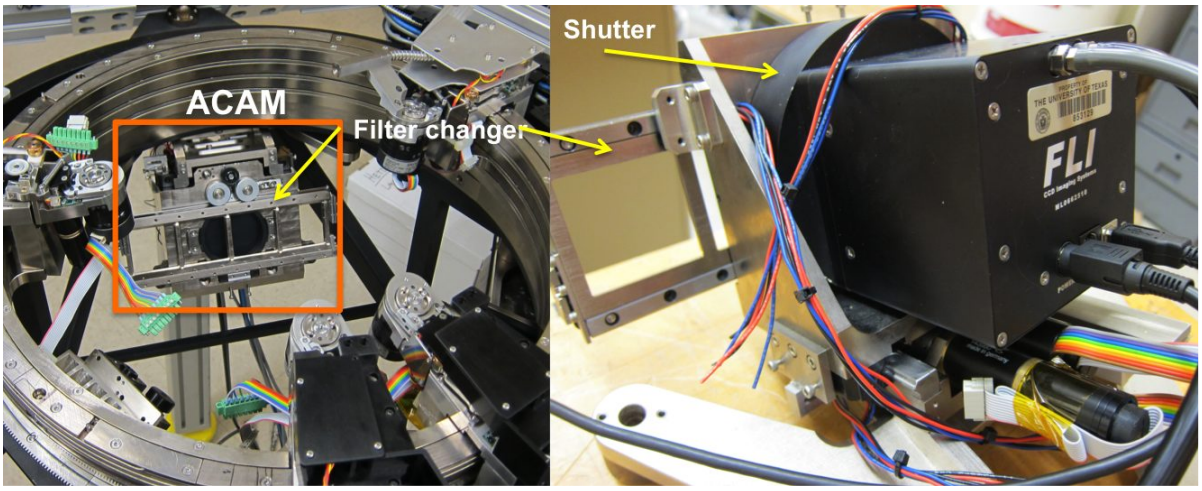

Figure 17 Acquisition Camera. (Left) ACAM assembled under the GP/WFS assembly, (Right) The rear view of the ACAM.

The ACAM (Figure 17) is located beneath the GP/WFS assembly and contains a FLI ML090000 that uses a Kodak KAF-09000 monochromatic 16-bit CCD chip with liquid-cooled TEC. The pixel format is 3056x3056 with 12µm pitch. The pixel scale is 0.068 arc-seconds and we plan to bin it by 4. It has a 3.5 arc-minutes field of view about the center of the telescope field. The camera is fed light by a pneumatically deployed fold mirror (not shown in the picture but see Ref. [12]) located opposite to the ACAM underneath the GP/WFS assembly. When the ACAM is used, the pick-off mirror extends toward the center of the beam to re-direct the central portion of the field to the ACAM. The camera is able to focus +/-15mm from nominal along a pair of adjustable preload THK HR1530 ball guides. Actuation is by a miniature ball screw purchased from Misumi and turned by the Maxon ECmax 22 motor and gear head used in the guide probe assembly and elsewhere. A Lika linear magnetic absolute encoder with 5 microns resolution is used to measure focus position. Its SSI interface is connected directly to the Maxon EPOS2 motor controller for position control. The acquisition camera includes a four-position filter changer for 50mm square filters. The filter changer rides on a set of adjustable preload ball guides purchased from Misumi. A toothed belt is stretched along one edge of the magazine and through two idlers and a drive pulley. The drive pulley is turned by one of the same Maxon motor and gear heads. Four hall effect switches are mounted to the chassis and triggered by two magnets on the filter magazine. Each hall effect switch corresponds to a filter position and their outputs are wired to the Maxon motor controller. A homing mode is used to drive the magazine position until the desired hall effect switch is triggered. Owing to its relatively large field of view, the ACAM is to be used for acquiring and identifying a science target field, which will be used to register the other facility instruments at the central port of the focal surface, namely the High Resolution Spectrograph, Medium Resolution Spectrograph, and Low Resolution Spectrograph-2. The ACAM can also provide imaging capability for different science observations. The ACAM will also be used to occasionally monitor the plate scale variation and the image quality of the telescope.

2.5 Pupil Viewing Camera (PVCam) and Calibration Wavefront Sensor (CWFS)

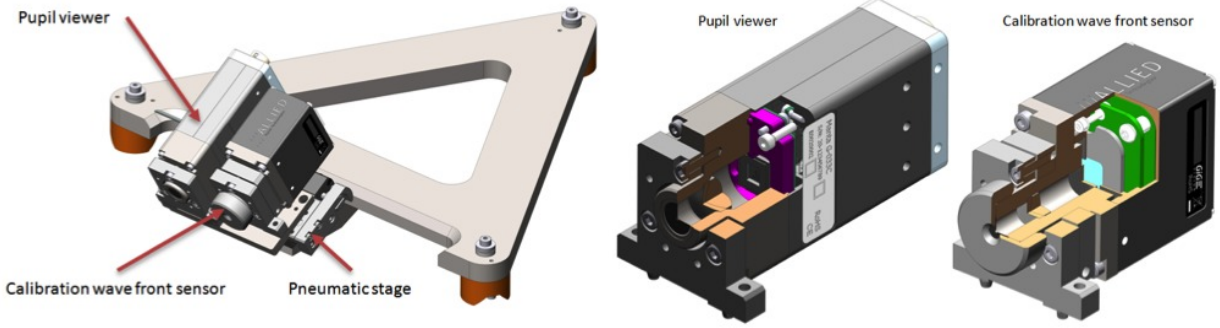

Figure 18 (Left) The PVCam and CWFS on their pneumatic stage. (Right) The section views of the solid models of the PVCam and CWFS.

The solid models of the PVCam and the CWFS are shown in Figure 18. Both optical metrology devices are located underneath the GP/WFS assembly. Both are built around AVT machine vision cameras. The pupil viewer has a collimating lens in custom housing mounted directly to a AVT Manta G-046 camera with stock C-mount bayonet removed. The CCD sensor uses a SONY ICX415 3 color 12-bit CCD chip. The pixel format is 780x580 with 8.3µm pitch. At the front of the PVCam, a field stop of 7 arc-seconds diameter is integrated in order to deal with a large pointing mismatch and at the same time to minimize stray-light into the system. The field stop is centered on the telescope field. The main function of the PVCam is to provide the image of the telescope pupil. The size of the re-imaged 10-m telescope pupil is 3.8mm in diameter on the CCD. This allows us to image individual M1 segments in three colors at a resolution of 50 pixels across mirror segment. Photometry of the segment images can give us the spectral response of the segments over time and the time-dependent mirror reflectivity degradation can be monitored in a relative sense from a particular point of time (e.g. when the segment is re-coated). Another function of the PVCam is to monitor the moving baffle that is mounted in the exit pupil at about half way between M5 and the focal surface. The the moving baffle blocks the section of the pupil falling outside the primary mirror during a track and it is important to test if the baffle follows the primary mirror during a track. In addition, the telescope pupil measurement during different sets of tracks will verify the telescope's dynamic obscuration model that has been derived from the HET WFU Zemax design and will be used in the calibration process of the HETDEX data.

The CWFS has a custom housing for collimating optics and micro-lens array mounted to a AVT Prosilica GC2450 camera. The CCD sensor uses a Sony ICX625 monochromatic 12-bit CCD chip. The pixel format is 2448x2050 with 3.5µm pitch. The CWFS field of view is 6.4 arc-seconds in diameter and centered on the telescope field. The CWFS uses a Fused-silica hexagonal miro-lens array with 250µm pitch. Each micro-lens is f/16 and the focal length variation is at 1% level. The projected size of the 10-m telescope pupil is 5.2mm in diameter or 21 sub-apertures across the diameter. Therefore, at least 100 sub-apertures are fully illuminated in any track positions, enabling us to sense telescope aberrations higher than what the WFS in the GP/WFS assembly can provide. The aberration data from the CWFS can then be used to calibrate the signal from the WFS. As shown in Figure 19, the sub-aperture size is chosen so that there is one sub-aperture at the border of two neighboring segments. This allows us to determine the inter-segment phase errors (via Broadband phasing algorithm[11]), which is used to verify the segment piston correction from the DMI. Details of segment phasing at the HET using the CWFS is being worked out at the time of this writing.

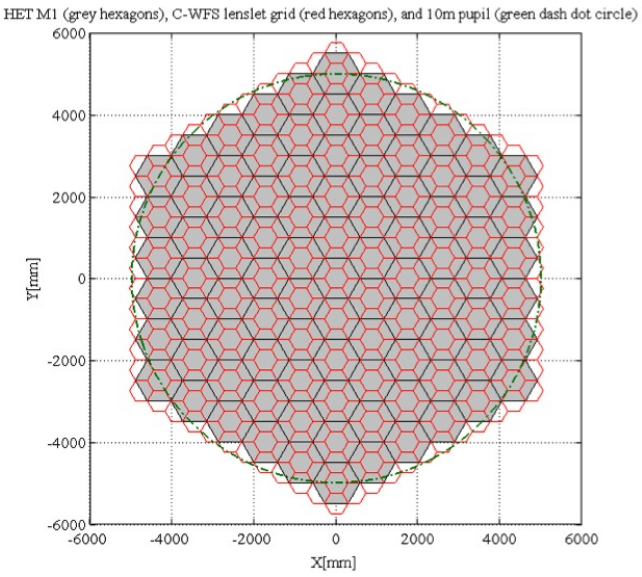

Figure 19 The sub-aperture grid of the CWFS overlaid on the HET Primary mirror segments.

Both the PVCam and CWFS use gigabit Ethernet communications and are air-cooled. The two devices are mounted to a Festo SLF-10 pneumatic slide to share the optical feed from a pneumatically deployed fold mirror (Figure 18, the mirror is not shown but see Ref. [12]). The pupil viewer has a tip-tilt-focus adjustable mount and the calibration wave front sensor has a tip-tilt-focus adjustment plus a rotational adjustment. A set of hall-effect switches detects position of the pneumatic stage at ends of travel.

3. METROLOGY FEEDBACK & CONTROL

From the metrology systems we will have sufficiently redundant information on the WFC alignment state with respect to the primary mirror. However, there is a fundamental difference between these metrology feedbacks. TTCam and DMI will provide the mechanical alignment state of the WFC, while the GP and WFS will produce the WFC alignment control feedbacks based on optical measurements (thus yielding the optical alignment state of the WFC). Although both TTS and DMI are to be calibrated against the optical measurement by the WFS and GP so that the relation between the optical axes of TTS and DMI and those of the WFC will be known, there is a possibility that this relationship changes during the operation of the telescope due to, for example, misalignment of the internal components of the WFC (i.e. the WFC mirrors and focal plane assembly). The WFC internal components are to be rigidly mounted to their mounting structure, but the Finite-Element Analysis of the WFC suggests that the internal mirrors and focal plane will be shifted and rotated due to variations in gravity vector and temperature during telescope operations. The internal alignment variations are expected to be repeatable so that they can be explicitly modeled or measured and then subtracted. In a situation where this is not the case due to the existence of unknown (or less accurate) telescope mount models, the WFS feedback will be used to set the fiducials of the DMI and TTS. Each metrology system will have different update rates. The TTS and DMI will have an update rate of 10 sec. The GP update rate can be made as fast as 1 ~ 5sec. The current baseline WFS update rate is 60 sec for an m_V=18 star. For brighter stars, the WFS update can be more frequent, but we plan to have the exposure longer than 15 seconds in order to sufficiently average out atmospheric aberrations which we do not wish to sense with the WFS. Given these differences between the metrology systems, it is necessary to coordinate the feedbacks from different metrology systems in order to optimally control the WFC alignment. The chart in Figure 20 illustrates the current snapshot of the metrology feedback and control. In the control flow, there are three primary "fast" control loops running on the Payload Alignment System (PAS) computer: DMI, tip/tilt, and guide. These loops run in parallel, asynchronously, with no cross dependencies. The DMI loop reads the distance measuring interferometer to maintain the distance from the WFC/PFIP to the primary mirror. The tip/tilt loop uses the TTCam to maintain the orientation of the WFC/PFIP mechanically with respect to the primary mirror. The guide loop keeps the WFC/PFIP pointed at the target star. A slower WFS loop uses wavefront sensing to check the focus and orientation of the WFC/PFIP optically and then adjusts the offsets in the DMI and tip/tilt loops. Each time the PAS takes an image from a camera, or reads the DMI, the data are processed locally and, for example, centroids are computed. These measurements are pushed onto a queue, which is in turn read by the Telescope Control System (TCS). The raw measurements are calibrated and

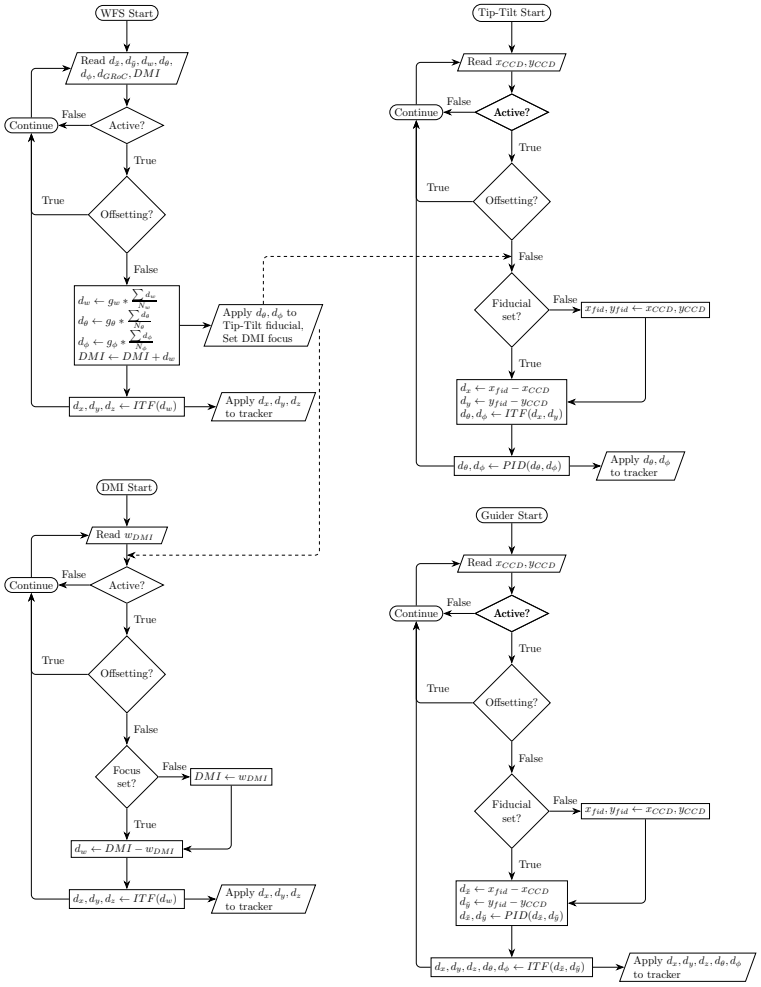

Figure 20 The metrology feedback and control flow diagram.

transformed geometrically into corrections to be applied to the tracker's trajectory. New sets of trajectory points are uploaded to the tracker on approximately 1-second intervals. As new metrology data come in on slower cadences, these points are recomputed using a simple running mean "predictive guiding" algorithm. Also, in parallel with the position and orientation data, photometric measurements from the guiders are piped to the GUI to tell the operator about current conditions, and to the science headers, to permit proper scaling of the frames making up a science dither set.

4. ON-SKY PERFORMANCE

Over the past few years, the individual HET metrology instruments have been constructed and tested in Austin lab and on-sky commissioned in 2016 and early part of 2017. The HET metrology instruments include two WFS, two Guide Probes (GP), a Tip/Tilt camera (TTCam), and a Distance Measuring Interferometer (DMI). The WFS and GP are the ones that measure the telescope pointing and alignment through the entire optical chain of the telescope. Their update rates are 15sec and 5sec, respectively. The TTCam and DMI measure the telescope's mechanical alignment at much higher frame rates. Together, these instruments provide redundant information on the telescope alignment.

The software effort has been the major item since then in order to fine tune the loop behavior of alignment control of the telescope using all information coming from these metrology instruments. The main alignment feedback comes from two WFS. These feedbacks are used within the TCS to guide the telescope alignment through a PID control loop. Since the update rate of the WFS is slower than TTCam and DMI, its alignment offset information is instead used to update the offset fiducial points for the DMI and TTCam, to which these instruments drive the telescope alignment.

One example of this combined control loop is shown in Figure 3. The WFS offset measured across little less than 2hr-long track shows well maintained focus (±12.5µm) and tip/tilt (±3 arcsec) alignment of the telescope at 1-sigma level. The typical guiding uncertainty is ±0.1 arcsec which translates to ±6.7µm rms in terms of the HET correct-M1 alignment. The sky rotation is constrained by our rho stage. The rho stage motion solely depends on the encoder value, but the rho angle stability is at the level that cannot be distinguished from guiding uncertainty. This demonstrates that the new HET alignment metrology hardware, software, and loop control algorithm are all implemented as intended. Also shown is the guider image quality that remains under 1.4 arcsec in FWHM over the entire track. The median image quality of the HET at the guider field (11 arcmin radial field) is 1.4 arcsec. Over this track, the HET pupil went through a substantial variation. Despite this, the numerical orthonormalization process in the WFS pipeline stabilized the aberration estimation process, that resulted in consistent telescope alignment offsets. Another WFS active alignment performance is shown in Figure 22 on a different night with similar behavior. Hence the suite of metrology instruments and their control loop are effectively keeping the telescope in alignment.

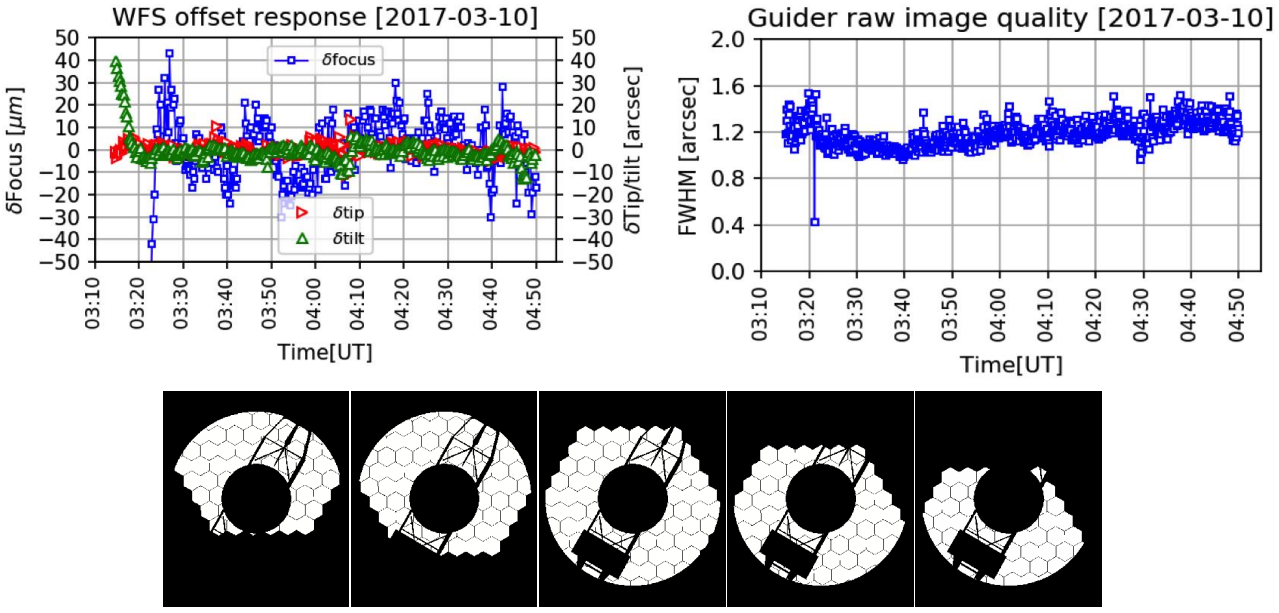

Figure **21** Example closed loop active alignment performance of the HET WFS on 2017-3-10 (Top Left) and the guider image quality in the full-width at half-max (FWHM) (Top Right). The HET pupil model over the track (Bottom)

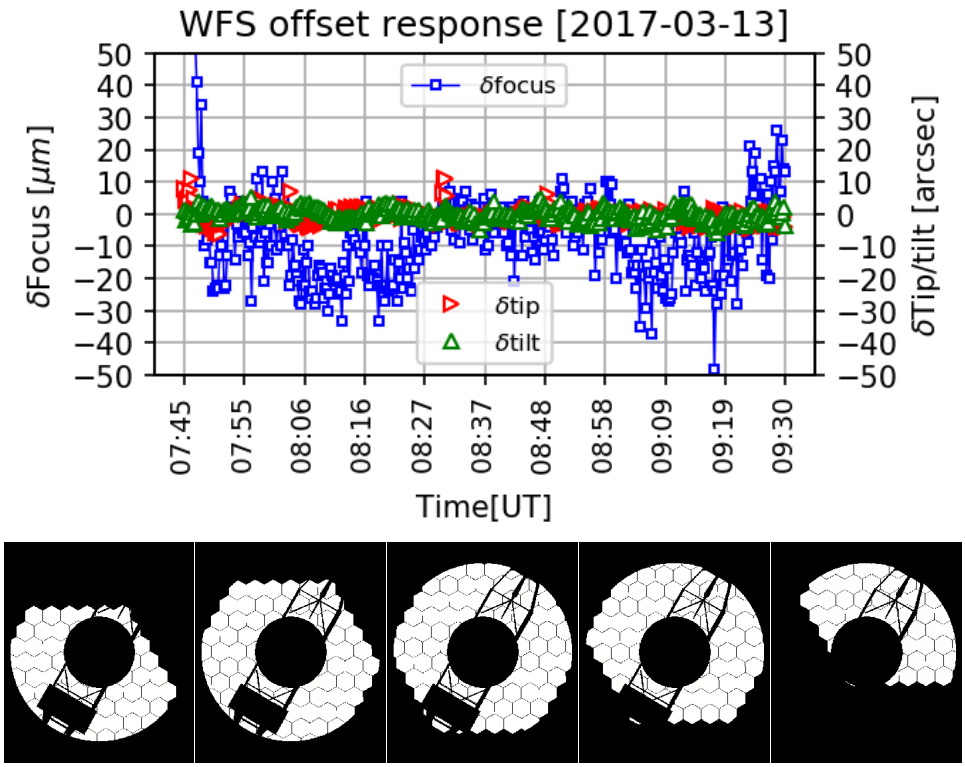

Figure **22** Another example of the closed loop active alignment performance of the HET WFS on 2017-3-13 (Top) and the corresponding HET pupil model (Bottom).

5. SUMMARY

Over the last few years, the individual metrology instruments have been constructed and tested in Austin lab and then on-sky commissioned in 2016 and early part of 2017. During the commissioning, the software effort has been the major item in order to fine tune the control loop behavior. The HET has been in science observing mode throughout the commissioning. Based on the commissioning data, the current active alignment control loop performance is as follows:

Table 2. The HET active alignment metrology control loop performance.

Alignment parameters	Decenter	Defocus	Tip/tilt	Rho
Performance	Better than 6.7μm	Better than 12.5μm	Better than 3arcsec	Better than 0.1arcsec
Requirement	±10μm	±10μm	±4arcsec	±20arcsec

The guider image quality also remains under 1.4 arcsec in FWHM over the example tracks. The median image quality of the HET at the guider field (11 arcmin radial field) is 1.4 arcsec. Hence the suite of metrology instruments and their control loop are effectively keeping the telescope in alignment. The new HET metrology system is functioning to the specification and currently supporting science programs using the HET Low Resolution Spectrograph 2, VIRUS, and Habitable-zone Planet Finder.

ACKNOWLEDGEMENTS

HETDEX is run by the University of Texas at Austin McDonald Observatory and Department of Astronomy with participation from the Ludwig-Maximilians-Universität München, Max-Planck-Institut für Extraterrestriche-Physik (MPE), Leibniz-Institut für Astrophysik Potsdam (AIP), Texas A&M University, Pennsylvania State University, Institut für

Astrophysik Göttingen, University of Oxford and Max-Planck-Institut für Astrophysik (MPA). In addition to Institutional support, HETDEX is funded by the National Science Foundation (grant AST-0926815), the State of Texas, the US Air Force (AFRL FA9451-04-2-0355), and generous support from private individuals and foundations.

REFERENCES

[1] G. Hill, et al., "Completion and performance of the Hobby-Eberly telescope wide field upgrade," Proc. SPIE, **10700-20** (2018).
[2] G. J. Hill, et al., "The Hobby-Eberly Telescope Dark Energy Experiment," AIP Conference Proceedings, 773 224-223 (2004).
[3] H. Lee, et.al, "Delivery, Installation, On-sky verification of the Hobby-Eberly Telescope wide-field corrector", Proc. SPIE, **7733**-51 (2010).
[4] H. Lee, et al., "Metrology systems for the active alignment control of the Hobby-Eberly Telescope wide-field upgrade," Proc. SPIE, 9906-46 (2016).
[5] P. Palunas, et al., "Imaging performance of the Hobby-Eberly Telescope," Proc. SPIE **6267**-127 (2006).
[6] M. T. Adams, et al., "Hobby-Eberly Telescope Segment Alignment Maintenance System," Proc. SPIE **4837,** 693-701 (2003).
[7] M.J. Wolf, M. Ward, J.A. Booth, A. Wirth, G.L. Wesley, D. O'Donoghue, & L. Ramsey, "Mirror Alignment Recovery System on the Hobby-Eberly Telescope", in Large Ground-Based Telescopes, Proc SPIE 4837, 714, 2003.
[8] Fogale Nanotech, "Low coherence interferometric sensor, Model: LISE-LS 40, HET 2Channel," User's Manual (2005).
[9] J.D. Murphy, G.J. Hill, P.J. MacQueen, T. Taylor, I. Soukup, W. Moreira, M.E. Cornell, J. Good, S. Anderson, L. Fuller, H. Lee, A. Kelz, M. Rafal, T. Rafferty, S. Tuttle, & B. Vattiat, "The Effects of Motion and Stress on Optical Fibers", Proc. SPIE, 8446-207 (2012).
[10] H. Lee, Gary J. Hill, Michael Hart, and Marc D. Rafal, "Analysis of active alignment control of the Hobby-Eberly Telescope Wide Field Corrector using Shack-Hartmann wavefront sensors," Proc. SPIE, **7738**-18 (2010).
[11] Gary Chanan, Mitchell Troy, Frank Dekens, Scott Michaels, Jerry Nelson, Terry Mast, and David Kirkman, "Phasing the Mirror Segments of the Keck Telescopes: The Broadband Phasing Algorithm," Applied Optics, **37**, 140-155 (1998).
[12] B.L. Vattiat, G.J. Hill, H. Lee, D.M. Perry, M.D. Rafal, T. Rafferty, R. Savage, C.A. Taylor III, W. Moreira, M.P. Smith, "Design, testing, and performance of the Hobby Eberly Telescope prime focus instrument package," Proc. SPIE, 8446-269 (2012).
[13] H. Lee, Gary J. Hill, and Michael Hart, "Phase retrieval analysis of the Hobby-Eberly Telescope primary mirror segment surface error and its implications for the wavefront sensing in the new wide-field upgrade," Proc. SPIE, **7738**-58 (2010).